Microstructure and hardness of SAC305 and SAC305-0.3Ni solder on Cu, high temperature treated Cu, and graphene-coated Cu substrates

Li, Shengli; Liu, Yang; Zhang, Hao; Cai, Hongming; Sun, Fenglian; Zhang, Guoqi

DOI
10.1016/j.rinp.2018.10.005

Publication date
2018

Document Version
Final published version

Published in
Results in Physics

Citation (APA)
Li, S., Liu, Y., Zhang, H., Cai, H., Sun, F., & Zhang, G. (2018). Microstructure and hardness of SAC305 and SAC305-0.3Ni solder on Cu, high temperature treated Cu, and graphene-coated Cu substrates. *Results in Physics*, *11*, 617-622. https://doi.org/10.1016/j.rinp.2018.10.005

Results in Physics 11 (2018) 617–622

Contents lists available at ScienceDirect

Results in Physics

journal homepage: www.elsevier.com/locate/rinp

Microstructure and hardness of SAC305 and SAC305-0.3Ni solder on Cu, high temperature treated Cu, and graphene-coated Cu substrates

Shengli Li[a], Yang Liu[a,b,*], Hao Zhang[a,b], Hongming Cai[a], Fenglian Sun[a], Guoqi Zhang[b]

[a] School of Materials Science and Engineering, Harbin University of Science and Technology, Harbin, China
[b] EEMCS Faculty, Delft University of Technology, Delft, Netherlands

A R T I C L E I N F O

Keywords:
Sn-Ag-Cu
Microstructure
Hardness
Graphene
Soldering

A B S T R A C T

In this study, SAC305 and SAC305-0.3Ni solder balls were soldered onto Cu, high temperature treated Cu (H-Cu) and graphene coated Cu (G-Cu) substrates, respectively. The microstructure, the interfacial reaction, and the hardness of the solder joints were investigated. The interfacial intermetallic compound (IMC) is Cu_6Sn_5 in the solder joints of SAC305/Cu, SAC305/H-Cu, and SAC305/G-Cu. With the addition of 0.3 wt% Ni in the SAC305 solder, the interfacial IMC on Cu, H-Cu, and G-Cu transforms from Cu_6Sn_5 into $(Cu, Ni)_6Sn_5$. The thickness of Cu_6Sn_5 and $(Cu, Ni)_6Sn_5$ is the lowest on G-Cu substrate. Meanwhile, smooth $(Cu, Ni)_6Sn_5$ interfacial IMC layers are obtained in SAC305-0.3Ni/H-Cu and SAC305-0.3Ni/G-Cu solder joints. Both the SAC305 and the SAC305-0.3Ni solder bulks have the highest β-Sn content and the lowest concentration of eutectic phases on G-Cu substrate. Consequently, the hardness of the solder bulks on G-Cu is lower than that on the other two kinds of substrates.

Introduction

With the rapid development of electronic industry, miniaturization is the dominant trend of electronic devices. As the carrier of electrical, mechanical and thermal interconnection between components and substrate, the performance of the solder joint does not only directly affect the property but also affect long-time reliability of electronic products. For a solder joint, the interfacial reaction and IMC evolution between solder bulk and common substrates are critical issues to the reliability [1–3].

Sn-Ag-Cu (SAC) lead-free solder alloys are considered as promising candidates of Sn-Pb solder [4–6]. A series of publications have reported the researches of SAC solder on the common Cu substrate [7–10]. In order to improve the comprehensive properties of the SAC305 solder joints, a widely-used method is to add some additive elements into SAC305 solder alloy. Wang et al. [11] found that adding nano-SiO_2 into Sn3.0Ag0.5Cu solders improved the wettability and refined the microstructure of the SAC305 solder bulk. Chan et al. [12] indicated that the addition of Zn in the SAC solder restrained the growth of the interfacial intermetallic compound (IMC) layer. The lowest growth rate of the IMC was obtained when the concentration of Zn nanoparticles was 0.3 wt%. Gu et al. [13] added Co nanoparticles into SAC305 solder. The growth of the interfacial IMC layer was suppressed and the shear strength was improved due to the increasing Co content. The research by Li et al. [14] illustrated that the growth rate of Cu-Sn IMC decreased when Er element was added into SAC305 solder alloy. Yang et al. [15] discovered that the addition of Ag in the SAC solder alloy hindered the diffusion of the Cu atoms through the interface and suppressed the growth of the interfacial IMC layer.

The other way to improve the properties of the interfacial IMC layer is to modify the surface layer of the substrates or to use different types of substrates. Sn–Ag–Zn–In lead-free solder balls were soldered onto Ni substrate by Xu et al. [16]. Ni substrate had impacts on the microstructure of the solder bulk as well as the thickness of the interfacial IMC layer. Zou et al. [17] reported that the morphology of IMC layer transformed from the scallop layer into planar layer on Ag substrate. The tensile strength of the SAC/Ag_3Sn interface was lower than that of Ag/Ag_3Sn. Zhang et al. [18] demonstrated that the thickness of the interfacial IMC layer increased significantly by adding 0.5 wt% Ni into Cu substrate. Wang et al. [19] studied the thickness of Ni_3Sn_4 layer on the interfacial reaction between Sn-Bi alloy and Ni substrates. The thickness of the IMC layer was improved significantly when Ni content was up to 5%.

As introduced above, adding additive elements into solder alloy and modifying the constituent of substrates are effective methods to improve the reliability of solder joints. In this research, high temperature treatment and graphene-coating process were conducted to Cu substrate. The microstructure, IMC, and the hardness of SAC305 and

---

* Corresponding author at: School of Materials Science and Engineering, Harbin University of Science and Technology, Harbin, China.
E-mail address: lyang805@163.com (Y. Liu).

https://doi.org/10.1016/j.rinp.2018.10.005
Received 27 August 2018; Received in revised form 7 October 2018; Accepted 7 October 2018

SAC305-0.3Ni solder joints on Cu, high temperature treated Cu (H-Cu), and graphene-coated Cu (G-Cu) substrates were studied.

Experimental procedure

SAC305 and SAC305-0.3Ni solder alloys were melted into solder balls with the diameter of 1.6 mm. SAC305 and SAC305-0.3Ni solder balls were soldered onto Cu, H-Cu and G-Cu substrates under 260 °C for 60 s on a heating platform. In order to obtain G-Cu substrate, Cu substrate was heated up to 1000 °C in a heating furnace with the gases of Ar (300 sccm) and H_2 (50 sccm) for 30 min. Next, the gases of CH_4 (5 sccm), Ar (500 sccm), and H_2 (50 sccm) were injected into the furnace for 8 min. In the end, the Cu substrate was cooled naturally with the gases of Ar (300 sccm) and H_2 (50 sccm). The experimental procedure of H-Cu substrate was similar to the preparation of G-Cu substrate. Firstly, Cu substrate was heated up to 1000 °C in the heating furnace with the gases of Ar (300 sccm) and H_2 (50 sccm) for 30 min. Secondly, the gases of Ar (500 sccm) and H_2 (50 sccm) were injected into the furnace for 8 min. Finally, the Cu substrate was cooled with the gases of Ar (300 sccm) and H_2 (50 sccm).

The morphology and the constituent of the solder bulks and the interfacial IMC layer in the solder joints were investigated by FEI scanning electron microscope (SEM) and energy dispersive X-ray spectroscope (EDS). The average thickness of the interfacial IMC layers of six specimens was measured by the AutoCAD software. The hardness of the solder bulks was characterized by SHIMADZU DUH-211S nanoindentation teste and the hardness of the solder bulks was an average value of nine samples. Here, the loading speed was 4.9 mN/s, and the test force was 20 mN.

Results and discussion

Interfacial IMC of the solder alloy

Fig. 1 shows the cross-sectional morphology and EDS results of the interfacial IMC in the solder joints on Cu, H-Cu and G-Cu substrates. The interfacial IMC between SAC305 and three kinds of substrates are Cu_6Sn_5 according to the EDS results in Fig. 1(d), (e) and (f). As shown in Fig. 1(a), it is clear that the Cu_6Sn_5 layer has typical scallop morphology at the interface. As shown in Fig. 1(b), the thickness and the roughness of Cu_6Sn_5 solder layer on H-Cu substrate are thicker and smoother than that on Cu substrate. It is suggested that the structure of Cu substrate transforms from polycrystalline structure into single crystal structure after high temperature treatment. This phenomenon was approved by Tian et al. [20]. Their study indicated that the single crystal structure of Cu substrate affected the roughness of Cu_6Sn_5 layer. Meanwhile, the orientation of Cu_6Sn_5 grains was regular. Compared with SAC305/Cu and SAC305/H-Cu solder joints in Fig. 1(a) and (b), the thickness of Cu_6Sn_5 solder layer in the SAC305/G-Cu solder joint in Fig. 1(c) is lower than that of the other kinds of substrates. The growth of IMC layer in the SAC305/G-Cu solder joint is suppressed. As demonstrated by Chen et al. [21], the excellent protection performance of graphene-coated layer on G-Cu substrate prevented the surface of metal from oxidation. In addition, Ko et al [22] indicated that interfacial reactions and IMC growth was suppressed by graphene layer of Cu substrate. Therefore, the graphene-coated layer is also considered as a barrier to the interfacial diffusion. The growth of the interfacial IMC layers could be suppressed by this graphene layer.

The interfacial morphology and EDS results of SAC305-0.3Ni/Cu, SAC305-0.3Ni/H-Cu and SAC305-0.3Ni/G-Cu solder joints are shown in Fig. 2. As shown in Fig. 2(a), (b) and (c), the interfacial IMC transforms from Cu_6Sn_5 into $(Cu, Ni)_6Sn_5$ on all the three kinds of substrates with the addition of 0.3 wt% Ni in the solder alloy. This transformation is approved by the EDS results in Fig. 2(d), (e) and (f). As shown in Fig. 2(a), the IMC layer in the SAC305-0.3Ni/Cu solder joint is tiny $(Cu, Ni)_6Sn_5$ grains, among which there are many gaps. Compared with the Cu_6Sn_5 layer in Fig. 1(a), the thickness of the $(Cu, Ni)_6Sn_5$ interfacial IMC layer on Cu substrate is higher than that of the SAC305 solder layer on Cu substrate. As shown in Fig. 2(b), the solder joint of SAC305-0.3Ni/H-Cu has smoother and thinner IMC layer than that on Cu substrate. Compared with the $(Cu, Ni)_6Sn_5$ IMC layers on Cu and H-Cu substrates in Fig. 2(a) and (b), the thickness and the roughness of $(Cu, Ni)_6Sn_5$ layer in the SAC305-0.3Ni solder joints are lower on G-Cu substrate as shown in Fig. 2(c). This can be attributed to the graphene-coated layer on G-Cu substrate, which restrains the growth of the interfacial IMC. As shown in Fig. 1(c) and Fig. 2(c), smoother and thicker

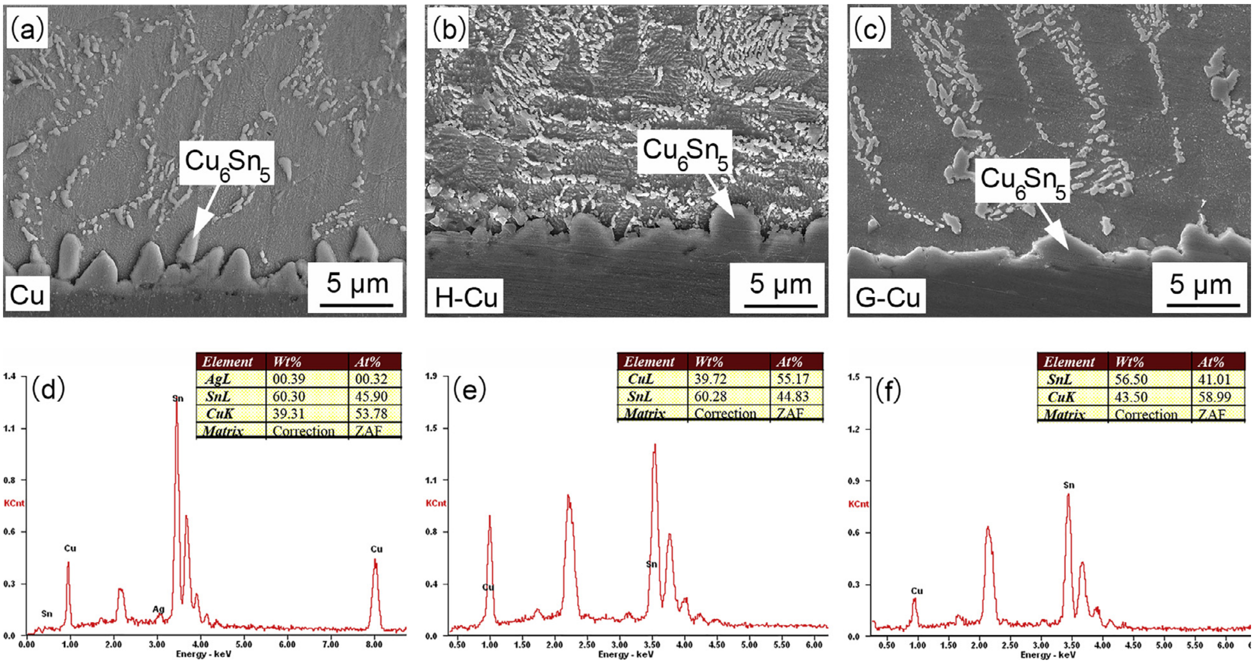

Fig. 1. SEM morphology and EDS analysis of the interfacial IMCs on the three substrates (a) SAC305 on Cu, (b) SAC305 on H-Cu, (c) SAC305 on G-Cu, (d) EDS of IMC in (a), (e) EDS of IMC in (b), (f) EDS of IMC in (c).

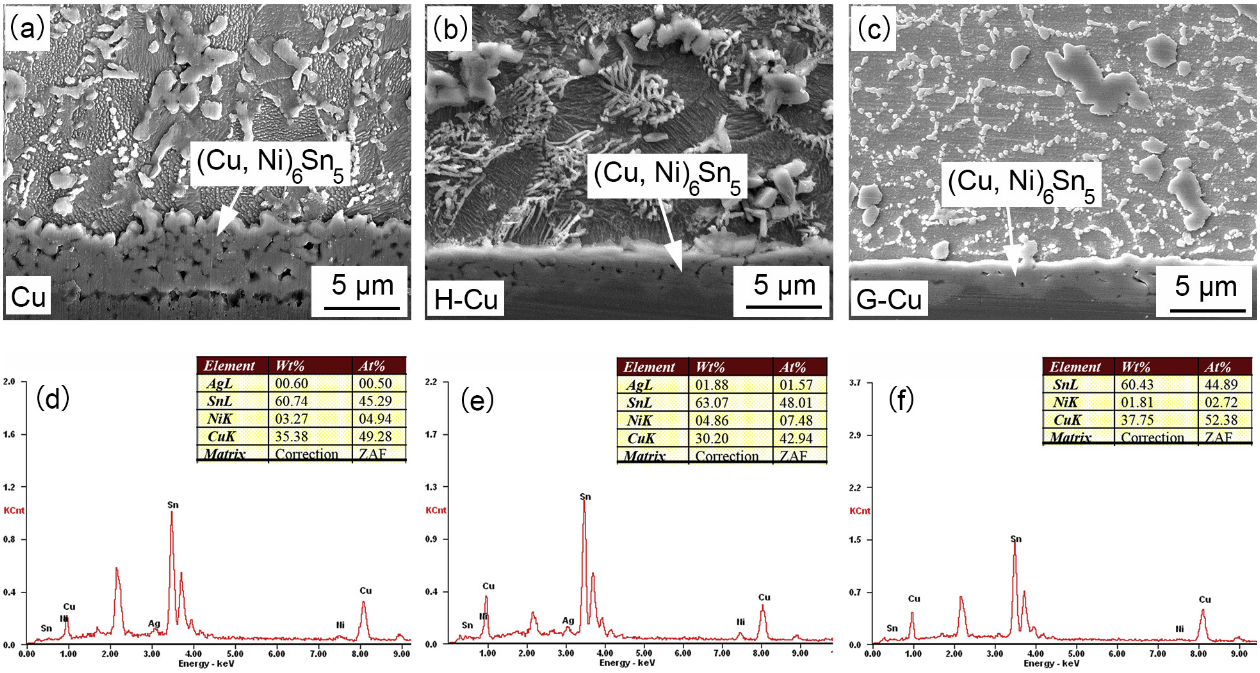

Element	Wt%	At%
AgL	00.60	00.50
SnL	60.74	45.29
NiK	03.27	04.94
CuK	35.38	49.28
Matrix	Correction	ZAF

Element	Wt%	At%
AgL	01.88	01.57
SnL	63.07	48.01
NiK	04.86	07.48
CuK	30.20	42.94
Matrix	Correction	ZAF

Element	Wt%	At%
SnL	60.43	44.89
NiK	01.81	02.72
CuK	37.75	52.38
Matrix	Correction	ZAF

Fig. 2. SEM morphology and EDS analysis of the interfacial IMCs on the three substrates (a) SAC305-0.3Ni on Cu, (b) SAC305-0.3Ni on H-Cu, (c) SAC305-0.3Ni on G-Cu, (d) EDS of IMC in (a), (e) EDS of IMC in (b), (f) EDS of IMC in (c).

(Cu, Ni)$_6$Sn$_5$ IMC layer in SAC305-0.3Ni solder joints is obtained when comparing with that in the solder joints of SAC305/G-Cu.

Fig. 3 shows the thickness of the interfacial IMC layers of SAC305 and SAC305-0.3Ni on Cu, H-Cu and G-Cu substrates, respectively. As shown in Fig. 3, the thickness of Cu$_6$Sn$_5$ solder layer in the SAC305/Cu solder joint is approximately 3.2 μm. With the addition of 0.3 wt% Ni in the SAC305 solder alloy, the interfacial IMC transforms from Cu$_6$Sn$_5$ into (Cu, Ni)$_6$Sn$_5$. Meanwhile, the thickness of the IMC layer of SAC305-0.3Ni solder on Cu substrate significantly increases to 6.31 μm. With the addition of 0.3 wt% Ni in the solder alloy, the thickness of the interfacial IMC layer rises from 2.84 μm to 4.16 μm on H-Cu substrate and the thickness of the interfacial IMC layer ranges from 1.7 μm to 3.0 μm on G-Cu substrate. As the (Cu, Ni)$_6$Sn$_5$ has more nucleation sites than Cu$_6$Sn$_5$, the (Cu, Ni)$_6$Sn$_5$ IMC layers are thicker than the Cu$_6$Sn$_5$ IMC layers. This phenomenon illustrates that the addition of 0.3 wt% Ni in the solder alloy increases the thickness of the IMC layers in the solder joints of SAC305-0.3Ni/Cu, SAC305-0.3Ni/H-Cu and SAC305-0.3Ni/G-Cu.

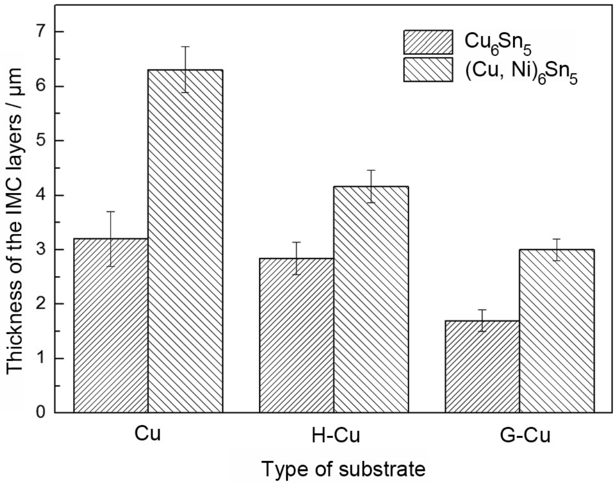

Fig. 3. Thickness of the IMC layers in the solder joints.

As shown in Fig. 3, compared with the thickness of Cu$_6$Sn$_5$ layer in the SAC305/Cu solder joint, it is clear that the thickness of Cu$_6$Sn$_5$ layer in the SAC305/H-Cu solder joint is thinner. This phenomenon is attributed to the changes of the crystal structure on H-Cu substrate after high temperature treatment. Meanwhile, the thickness of the interfacial IMC layer in the solder joint of SAC305/G-Cu is lower than that of SAC305 IMC layers on Cu and H-Cu substrates. On one hand, the crystal structure of Cu substrate transforms during the graphene-coating process. On the other hand, the coated-graphene layer on G-Cu substrate works as a diffusion barrier at the interface of the solder joint. Therefore, the growth of the interfacial IMC layer is suppressed significantly.

Microstructure of the solder bulks in the solder joints

Fig. 4 shows the microstructure of the solder bulks in the solder joints of SAC305/Cu, SAC305/H-Cu and SAC305/G-Cu. As shown in Fig. 4(a) and (d), the microstructure of the solder bulk in the SAC305/Cu solder joint consists of two parts, the β-Sn phase and the eutectic phase. As presented in Fig. 4(b), the grain shape of the β-Sn phase in the SAC305/H-Cu solder joint is longer than that on Cu substrate. Meanwhile, the β-Sn grains present regular orientation in the solder bulk on H-Cu substrate. As H-Cu substrate transforms to single crystal structure during the high temperature treatment, the growth of the β-Sn phase is affected by the crystal orientation of the substrate. As shown in Fig. 4(c), compared with the microstructure of the solder bulk on Cu and H-Cu substrates, the microstructure of the SAC305 solder bulk has higher β-Sn content and lower concentration of eutectic phases on G-Cu substrate. Meanwhile, the growth of the β-Sn grains does not grow along any orientation as that on H-Cu substrate.

Fig. 5 shows the microstructure of the SAC305-0.3Ni solder bulks on Cu, H-Cu and G-Cu substrates. As shown in Fig. 5, the microstructure of the SAC305-0.3Ni solder bulks on Cu, H-Cu and G-Cu substrates is composed of the β-Sn phase and the eutectic phase. As shown in Fig. 4(a) and Fig. 5(a), the grain size of β-Sn slightly decreases with the addition of 0.3 wt% Ni, but the area of β-Sn has limited change. Meanwhile, a small quantity of IMC phases in the solder bulk is found in the SAC305-0.3Ni/Cu solder joint. As shown in Fig. 5(b), with the addition of Ni in the SAC305 solder alloy, the microstructure of the

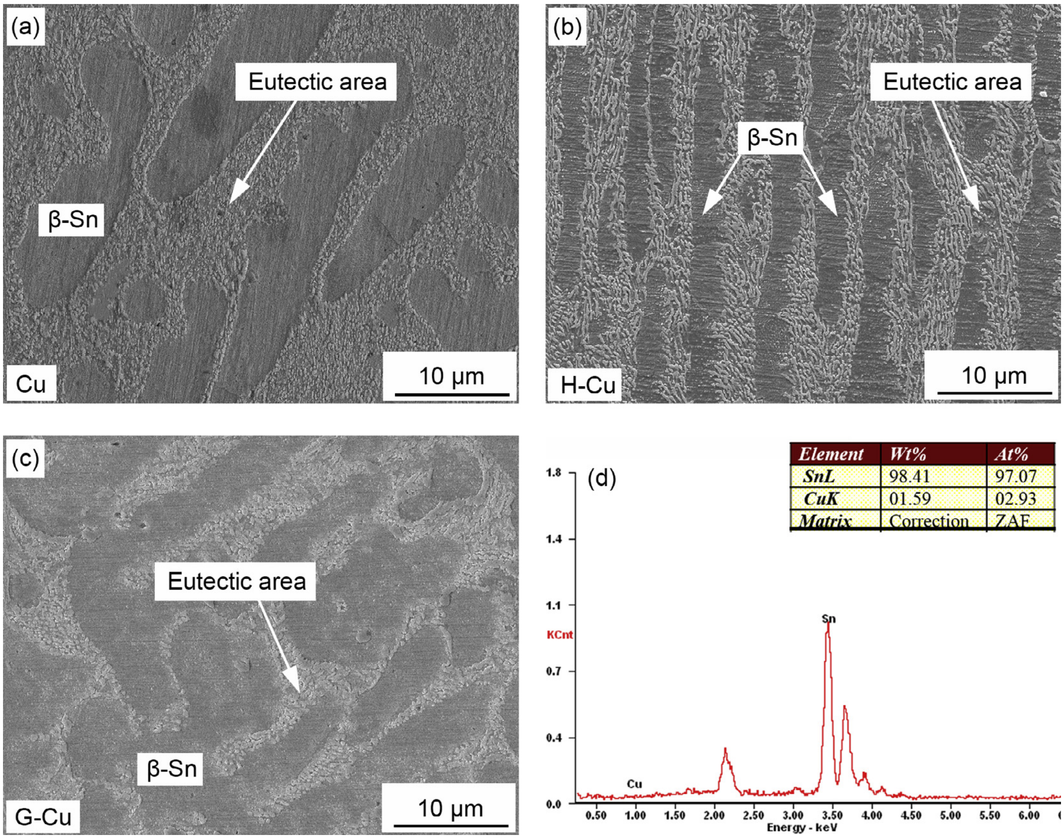

Element	*Wt%*	*At%*
SnL	98.41	97.07
CuK	01.59	02.93
Matrix	Correction	ZAF

Fig. 4. Microstructure of the solder bulks by SEM: (a) SAC305 on Cu, (b) SAC305 on H-Cu, (c) SAC305 on G-Cu, (d) EDS of β-Sn.

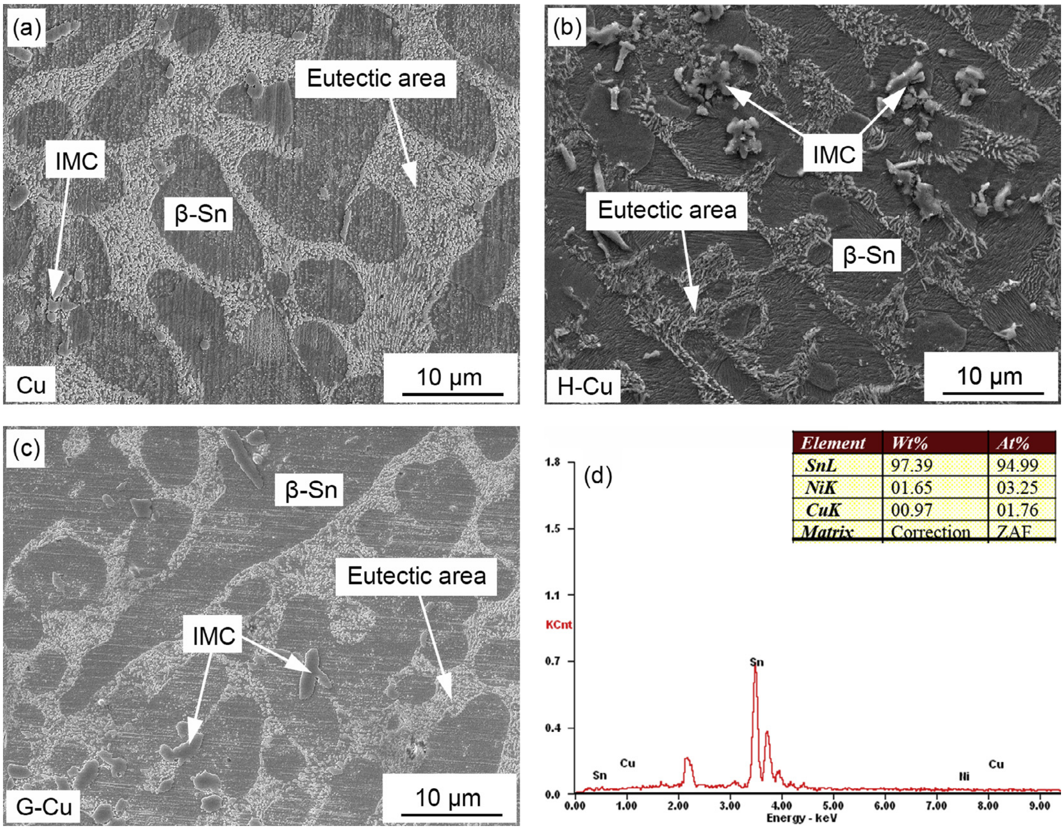

Element	*Wt%*	*At%*
SnL	97.39	94.99
NiK	01.65	03.25
CuK	00.97	01.76
Matrix	Correction	ZAF

Fig. 5. Microstructure of the solder bulks by SEM: (a) SAC305-0.3Ni on Cu, (b) SAC305-0.3Ni on H-Cu, (c) SAC305-0.3Ni on G-Cu, (d) EDS of β-Sn.

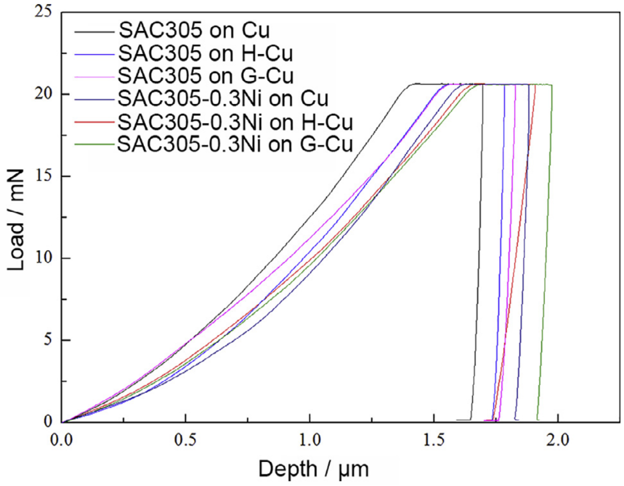

Fig. 6. Indentation and displacements of the solder bulks.

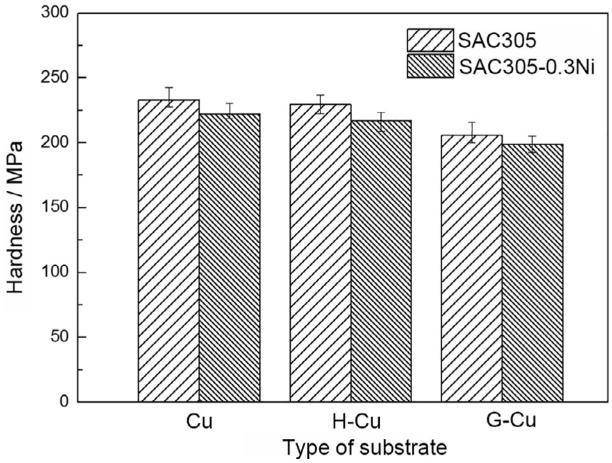

Fig. 7. Hardness of the solder bulks of SAC305 and SAC305-0.3Ni solders on the Cu, H-Cu and G-Cu substrates.

SAC305-0.3Ni solder bulk on H-Cu substrate has higher β-Sn content and lower concentration of eutectic phase than that in the SAC305/ H-Cu solder joint. The number of IMC phases increases due to the addition of Ni. Compared with the microstructure of the solder bulk in the SAC305/G-Cu solder joint in Fig. 4(c), the eutectic area of the SAC305-0.3Ni solder bulks decreases obviously and the grain size of β-Sn phase is smaller, as shown in Fig. 5(c). This is attributed to the fact that the addition of 0.3 wt% Ni in the solder alloy makes Cu_6Sn_5 in the eutectic phase of the solder bulk transform into $(Cu, Ni)_6Sn_5$ and the grain size of $(Cu, Ni)_6Sn_5$ is smaller than that of Cu_6Sn_5.

Hardness of solder bulks

Fig. 6 shows the load-depth relationships of SAC305 and SAC305-0.3Ni solder bulks on Cu, H-Cu and G-Cu substrates. As presented by the correlation curves in Fig. 6, the indentation depth of the solder bulk increases during the upload-process. The maximum load of this research is 20 mN. When the load force reaches 20 mN, the indentation depth of SAC305-0.3Ni solder bulks on Cu, H-Cu and G-Cu substrates is about 1.6 μm, 1.7 μm and 1.9 μm. Meanwhile, the depth of SAC305 on Cu, H-Cu and G-Cu substrates is about 1.25 μm, 1.35 μm and 1.5 μm, respectively. The result indicates that the indentation depth of the solder bulk in the SAC305-0.3Ni/G-Cu solder joint is the highest. The indentation depth of the SAC305 solder bulk on Cu substrate is the lowest in all the tested samples.

The hardness of SAC305 and SAC305-0.3Ni solder bulk on Cu, H-Cu and G-Cu is presented in Fig. 7. As shown in Fig. 7, the average hardness of the SAC305 eutectic solder bulk on Cu substrate is about 233.3 MPa. The hardness of the SAC305 eutectic solder bulks in SAC305/H-Cu and SAC305/G-Cu solder joint is about 229.6 MPa and 205.8 MPa, respectively. Compared with the microstructure of the SAC305 eutectic solder bulks on Cu and H-Cu substrates as shown in Fig. 4(a) and (b), the SAC305 eutectic solder bulk on G-Cu substrate has higher β-Sn content and lower concentration of eutectic phase in Fig. 4 (c). Since β-Sn is a soft phase, the hardness of the SAC305 solder bulk on G-Cu substrate is lower than that on the other two kinds of substrates. As presented in Fig. 7, the hardness of the solder bulk in the SAC305-0.3Ni/Cu solder joint is about 222.4 MPa, and the hardness of the solder bulk of SAC305-0.3Ni solders on H-Cu and G-Cu substrates decreases to 217 MPa and 198.8 MPa, respectively. The reason is similar to that of the SAC305 solder. As shown in the figure, another phenomenon is that the hardness of SAC305-0.3Ni solder bulk is slightly lower than that of SAC305 on the same substrate type. According to the microstructure in Fig. 4 and Fig. 5, the addition of Ni in the SAC305 solder leads to the refinement of β-Sn phase and the suppression of the eutectic phase. Therefore, the hardness of the solder bulk decreases.

Conclusion

1. Scallop-like Cu_6Sn_5 appears in the interfacial IMC of SAC305 on Cu, H-Cu and G-Cu substrates. Smooth IMC layers are obtained on G-Cu substrate. The thickness of the IMC layer on G-Cu substrate is lower than that on the other two kinds of substrates.
2. The interfacial IMC in the solder joints of SAC305-0.3Ni/Cu, SAC305-0.3Ni/H-Cu, and SAC305-0.3Ni/G-Cu is $(Cu, Ni)_6Sn_5$. Smooth IMC layers are obtained on H-Cu and G-Cu substrates. The thickness of the IMC on G-Cu is the lowest in all the three kinds of substrates.
3. Compared with the solder bulks of SAC305 on Cu, H-Cu, and G-Cu substrates, SAC305-0.3Ni has more refined β-Sn grains and lower concentration of eutectic phase. The hardness of SAC305-0.3Ni is slightly lower than that of SAC305 on the three kinds of substrates.
4. For both SAC305 and SAC305-0.3Ni, the solder bulks on G-Cu substrate have higher β-Sn content and lower concentration of eutectic phase than that on the other two kinds of substrates. The hardness of the solder bulks on G-Cu is the lowest.

Acknowledgement

This work is supported by National Natural Science Foundation of China (No. 51604090), Natural Science Foundation of Heilongjiang Province (No. E2017050), and University Nursing Program for Young Scholars with Creative Talents in Heilongjiang Province (UNPYSCT-2015042).

References

[1] Xu L, Pang JHL, Che F. J Electron Mater 2008;37:880–6.
[2] Sun F, Hochstenbach P, Driel WDV. Microelectron Reliab 2008;48:1167–70.
[3] Chin YT, Lam PK, Yow HK. Microelectron Reliab 2008;48:1079–86.
[4] Chellvarajoo S, Abdullah MZ. Mater Des 2016;90:499–507.
[5] Bukat K, Sitek J, Kościelski M. Solder Surf Mt Tech 2012;24:267–79.
[6] Chang SY, Tsao LC, Wu MW. J Mater Sci-Mater El 2012;23:100–7.
[7] Zhang XR, Yuan ZF, Zhao HX. Sci Bull 2010;55:797–801.
[8] Hu F, Yang S, Kang UB. J Mater Sci-Mater El 2015;27:1–6.
[9] Wei GQ, Huang YL. J Mater Sci: Mater Electron 2012;23:130–5.
[10] Chuang CM, Lin KL. J Eelectron Mater 2003;32:1426–31.
[11] Wang Y, Zhao X, Xie X. J Mater Sci-Mater El 2015;26:9387–95.
[12] Chan YH, Arafat M, Haseeb ASMA. Solder Surf Mt Tech 2013;25:91–8.
[13] Gu Y, Liu Y, Zhao XC. Mater Sci Forum 2015;815:97–102.
[14] Bin LU, Hui LI, Wang JH. J Cent South Univ 2008;15:313–7.
[15] Yang M, Ko YH, Bang JH. Mater Charact 2017;124:250–9.
[16] Xu RL, Liu YC, Han YJ. J Mater Sci-Mater El 2009;20:675–9.

[17] Zou H, Zhu Q, Zhang Z. J Alloy Compd 2008;461:410–7.
[18] Zhang X, Hu X, Jiang X. Appl Phys A-Mater 2018;124:315.
[19] Wang J, Liu HS, Liu LB. J Electron. Mater 2006;35:1842–7.
[20] Tian Y, Zhang R, Hang C. Mater Charact 2014;88:58–68.
[21] Chen S, Brown L, Levendorf M. ACS Nano 2010;5:1321–7.
[22] Ko YH, Lee JD, Yoon T. ACS Appl Mater Interfaces 2016;8:5679–86.